Modification the Band Gap of Nano Titanium Dioxide and Application Its Effectiveness on Photodegradation of 3- Methyl Phenol

Fouad Warid Mezaal
Ministry of Education, Open Educational College, Dhi Qar Study Center, Iraq

* Corresponding Author: **Fouad Warid Mezaal**

Article Info

E-ISSN: 3107-7137
Volume: 02
Issue: 04
Received: 05-05-2026
Accepted: 04-06-2026
Published: 03-07-2026
Page No: 34-42

Abstract
This study uses the sol-gel method to modify the band gap of titanium dioxide (anatase) by adding nitrogen atoms. By employing the sol-gel technique to modify the band gap of titanium dioxide (anatase), nitrogen atoms can be added. This will decrease the valence energy difference between the valence unit VB and the conduction band CB, facilitating the transfer of electrons from VB to CB. The formation of an (e-/h+) pair will be stimulated by the efficient absorption of photons of light equal to or greater than the line penetration energy. X-ray diffraction was used to determine the structure of the produced TiO_2 grains, atomic force microscopy was used to determine the particle size and distribution, and ATR-FTIR and UV-Vis spectroscopy were used to analyze the photocatalytic repulsion. The resulting pair (e-/h+) will produce (˙OH) radicals, which can effectively remove organic contaminants from the surface of the photocatalyzed TiO_2. The target load of the photocatalyst (TiO_2) was (0.10 - 0.83 g/L) to supervise its implementation based on the analysis of 3-methylcarbolic acid (TiO_2) before the specific water decomposition of the structure. The target load of (0.10 - 0.83 g/L) was to supervise its implementation based on the analysis of 3-methylcarbolic acid before the specific water decomposition of the structure. It was found that the most efficient pressure was directly proportional (0.43 g/L). The activities of titanium dioxide (octahydrate) and TiO_2 drug with filling gas were directed under the control of an ultraviolet sky light source and explicit isolation presence according to the same standard. The height indicates that the aversion (primary command kinetics of the aversive mind) is 4.69×10^{-6} mins per 1 for TiO_2 and 9.44×10^{-6} mins per 1 for oxygen-free TiO_2. The ratio of command kinetics is constant at 4.69×10^{-6} mins per 1 for TiO_2 and 9.44×10^{-6} mins per 1 for oxygen-free TiO_2.

DOI: https://doi.org/10.54660/IJBBR.2026.2.4.34-42

Keywords: N-doped-TiO_2, sol-gel method, photodegradation, photocatalysis, AFM, XRD

1. Introduction

Titanium dioxide (TiO_2) semiconductor photocatalysts appear to be the most attractive option for environmental cleanup due to their numerous desirable properties. The only drawback of TiO_2 semiconductors is that they absorb a small amount of helical appearance in the ultraviolet range (the bandgap strength of octahedral TiO_2 is 3.2 eV, 384 nm, and 3.02 eV, 411 nm for rutile TiO_2). Consequently, in order to maximize the helix lifespan, management must continue to focus on the megastations [1-3]. Modifying titanium dioxide to increase its sensitivity to phenotypic life has become one of the most important tasks for advancing the use of titanium dioxide. Strategies for achieving this goal have been proposed. To improve visible light absorption, studies have looked into doping TiO_2 with transition metals like iron, nickel, and chromium. However, these doped materials contain more charge carrier recombination centers and are thermally unstable [4]. Atoms such as N [5, 6], S [7], and C [8] have been doped into TiO_2. There are three main fundamental perspectives on the mechanism of nitrogen-doped titanium dioxide modification.

1. **Band Gap Shortening:** The N2p hybrid states with the O2p states in nitrogen-doped TiO_2 anatase were identified because their energies are relatively similar, which narrows the band gap of N-TiO_2 and allows it to absorb visible light [9-10].
2. **Impurity Energy Levels:** Discrete impurity energy levels above the valence band are produced when nitrogen atoms are substituted for oxygen sites in TiO_2. Electrons in both are excited when exposed to UV light [11].
3. Oxygen-deficient sites created at grain boundaries are necessary for the appearance of visible activity, and nitrogen supplied to some of the oxygen-deficient sites is crucial as a redox barrier, according to the research of oxygen gaps [12].

The sol-gel process is used to modify the band gap of TiO2 semiconductors. The sol-gel synthesis process is based on the concept of "dissolving" a component in a liquid and then reconstituting it into a solid under controlled conditions. The sol-gel process is versatile and can be used to create any oxide composition, as well as some non-oxide compounds and organic-inorganic hybrids. Thanks to the high purity of the molecular mixture, no melting point is required, and a dense network structure can be achieved at low temperatures. Applications include films and coatings, homogeneous masses, composites, porous membranes, powders, and fibers. No specialized or expensive equipment is needed [13].

A molecule absorbs photons in the first step of the photocatalysis process, creating extremely reactive, electrically excited states. This absorption of photons by a molecule results in extremely reactive, electrically stimulated states in photocatalysis. The photon energy (h^2) needs to be at least as high as the semiconductor's band gap energy. An electron is excited from the valence band to the conduction band by the energy received, leaving the valence band with a positive hole. Negatively charged electrons and positively charged holes, or (e-/h+) pairs, are produced by this electron migration. Negatively charged electrons in the conduction band are efficient reducing agents, whereas positively charged holes in the valence band are potent oxidizing agents [14]. Strong oxidation occurs when electrons and holes transform nearby oxygen or water molecules into free radicals (OH^-). Many different chemical compounds, including certain metals, can be oxidized by them. Hazardous substances including benzene, formaldehyde, and ammonia can also be deoxidized using this method to produce carbon dioxide and water that are devoid of poisons, harm, and offensive odors [15]. Fig 1.

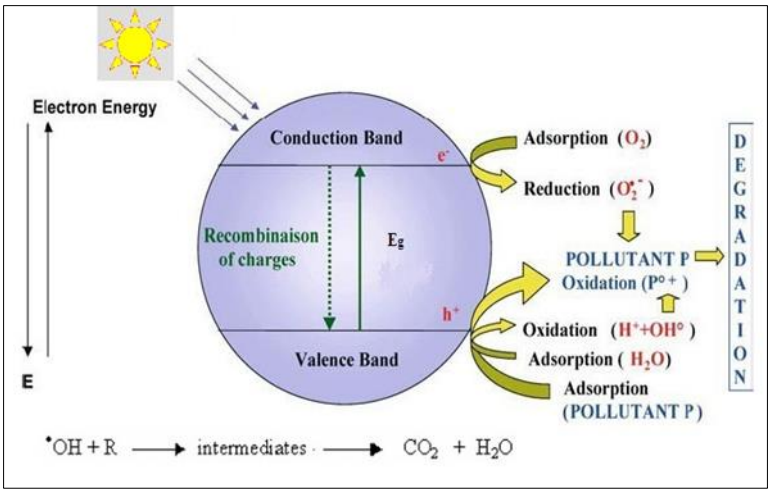

Fig 1: The principle of TiO2 photocatalysis.

2. Materials and Methods

Nitrogen-doped TiO2 photocatalysts were discovered using a sol-gel process. Initially, 5.00 mL of 35% ammonia, interpreted as a nitrogen spring, was continuously introduced into 10.00 mL of titanium tetraisopropoxide (IV), the titanium indicator, under continuous stirring (400 rpm) at 303 K. Rapid hydrolysis and condensation reactions resulted in a denser, colloid-like solution within the first ten minutes of addition. The system was kept in a coupling state at 303 K. To collect the residual ammonia discharge and certain organic byproducts from reverse hydrolysis, the creamy gel layer was kept and dried for an hour at 393 K in an oven [16]. In order to show hot breakdown, phase transformation, and the elimination of a volatile fraction, the produced N-fool TiO2 was finally calcined for an hour at different temperatures (573 K–1173 K) in a reflecting calciner while wearing a blindfold. The oxidation temperature has a significant impact on the color of nitrogen-doped titanium dioxide.

2.1. XRD

High-intensity monochromatic Cu K radiation (λ = 0.154056 nm) is used by the Holland Philips Xpert X-ray powder diffraction (XRD) apparatus at a scanning speed of 2"/min from 10" to 60" (2θ).

2.2. AFM

It is a device that identifies or captures an image of particles, as well as their size in three dimensions (x, y, z). It also determines the particle size distribution. Angstrom Advanced, USA. Model scanning probe microscope aa 3000A.

2.3. ATR-FTIR, UV-Vis

ATR-FTIR Bruker Model Tensor 27, Double+90Plus UV-Visible Spectrophotometer, PG Instrument Ltd.

3. Results and Discussion

Characterization of Synthetic Nanoparticles: Titanium dioxide (anatase) nanoparticles and nitrogen-doped titanium dioxide nanoparticles were analyzed using a Holland Philips Xpert X-ray diffraction (XRD) spectrometer. The particles were analyzed using a Holland Philips Xpert powder XRD spectrometer, as shown in Figure 2(a, b). Compared to the conventional results, the X-ray diffraction showed the following. The conventional X-ray diffraction results showed the following. Figure (2-a) shows the X-ray diffraction of titanium dioxide (anatase). The main peak intensity at 2ι=25.3455 is 100%, with other peaks at 2ι=37.8298, 48.0772, 53.9206, and 55.1004. Titanium dioxide (anatase) diffraction. The main peak at 2ι = 25.3455 exhibits 100% intensity, with other peaks at 2ι = 37.8298, 48.0772, 53.9206, and 55.1004. Figure (2-b) shows the X-ray diffraction of nitrogen-doped TiO2, with a main peak at (2ι = 25.7175) at 100% intensity and peaks at 2ω = 38.1511, 48.4860, 54.2079, and 55.3687.

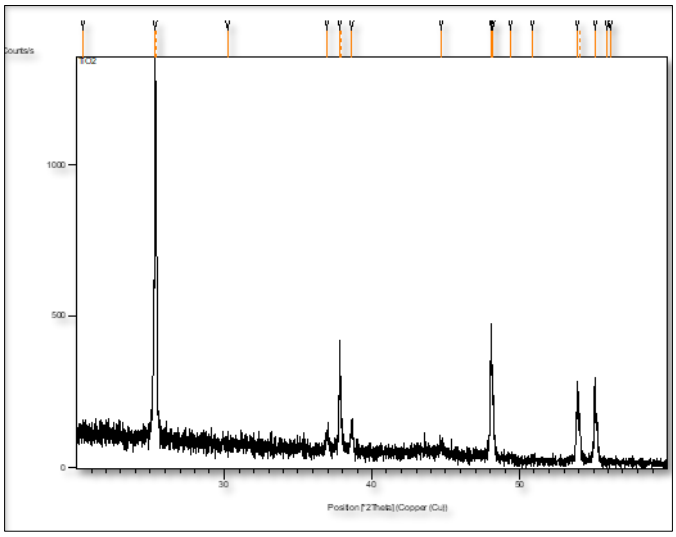

Fig 2: XRD pattern for TiO2 (anatase)

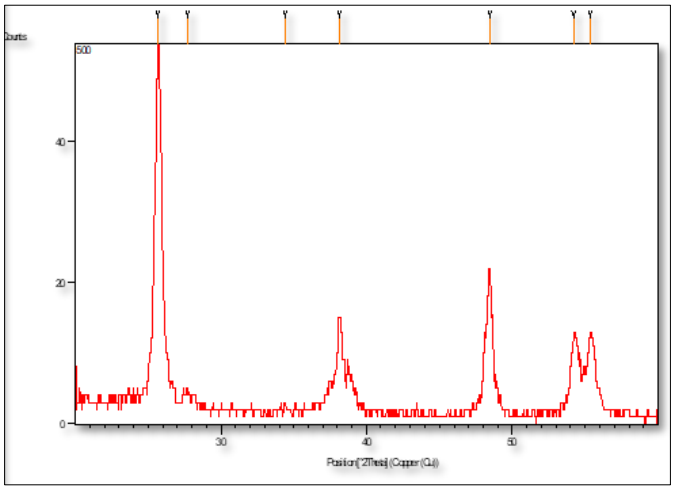

Fig 3: XRD pattern for N- doped TiO2

AFM spectra revealed a particle size distribution ranging from 60 to 135 nm for TiO2(anatase) and from 50 to 150 nm for nitrogen-doped TiO2 produced at 873 K. According to the findings, nitrogen-doped TiO2 has the biggest surface area, while TiO2 (anatase) has a decreased surface area as particle size decreases.

that illustrate in following figures :

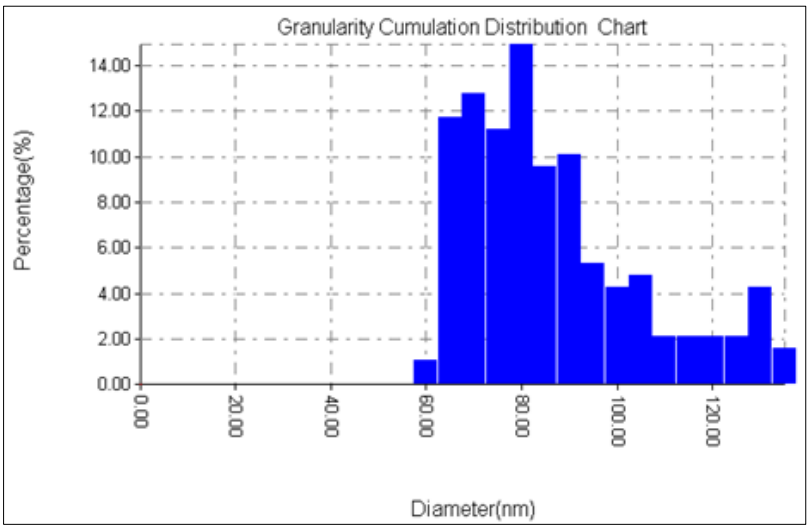

Fig 4: size distribution using AFM for the catalyst TiO2 (anatase) particle.

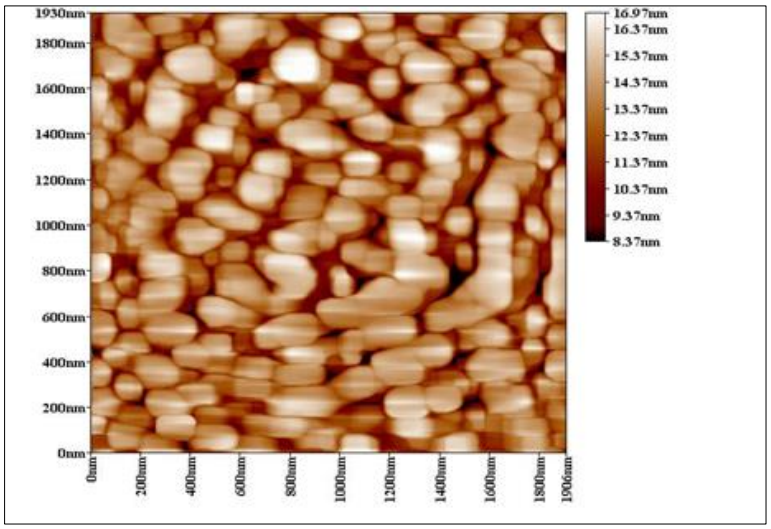

Fig 5: produced particles drawn by AFM on the X-Y axis catalyst TiO2 (anatase).

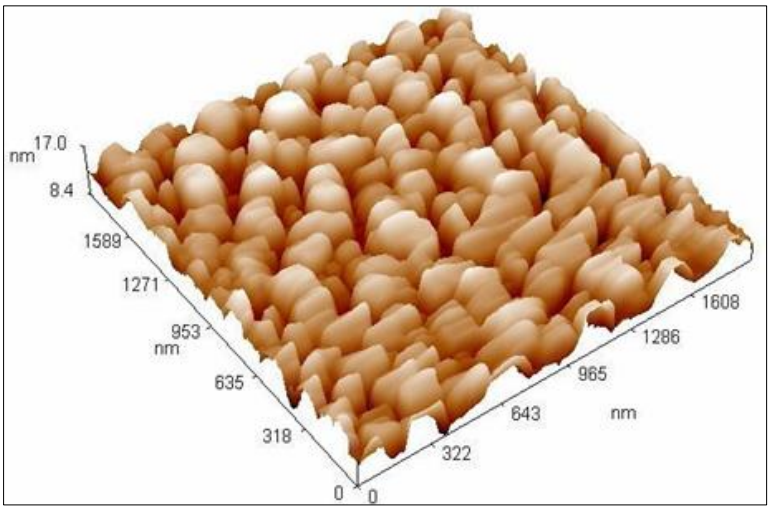

Fig 6: AFM-drawn prepared particles for the catalyst TiO2 (anatase) on the X, Y, and Z axes.

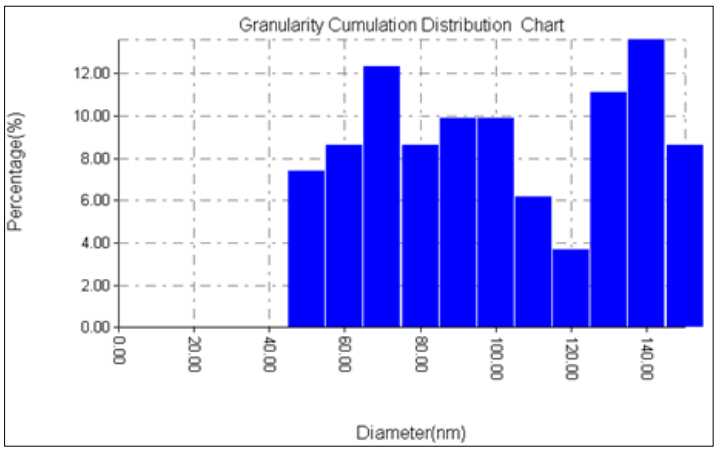

Fig 7: size distribution using AFM for catalyst nitrogen-doped TiO2 particles.

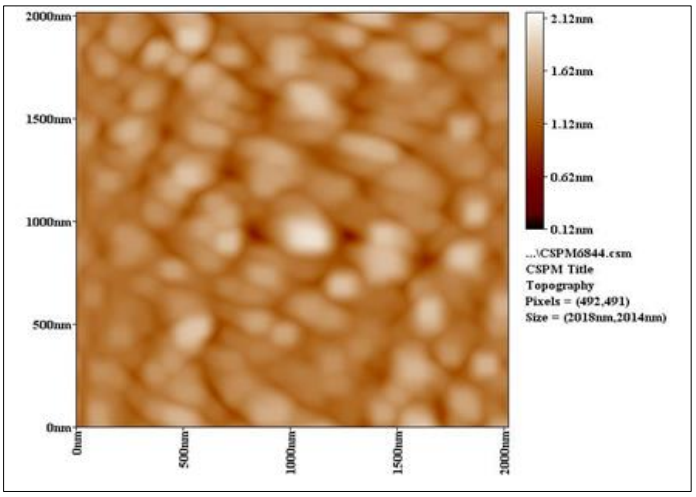

Fig 8: AFM-prepared particles for catalyst nitrogen-doped TiO2 were sketched on the X-Y axis.

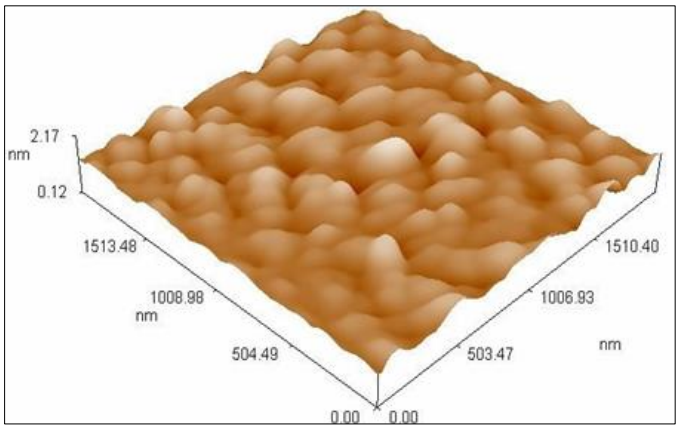

Fig 9: AFM-drawn produced particles for the catalyst nitrogen-doped TiO2 on the X, Y, and Z axes.

3.1. ATR-FTIR spectrum

Figure 10, the results demonstrate that the low frequency bands at 500 cm-1 are associated with the Ti-O-Ti bond vibration of the TiO2 catalyst (anatase).

Figure 11 shows the nitrogen-doped TiO2 catalyst at a drying temperature of 120 °C. Some of the peaks between 3243 and 1633 cm^{-1} are attributed to water and hydroxyl groups. The nitrogen atoms being substituted in the TiO2 lattice are responsible for the peak at 1438 cm^{-1}, which results from the bending of NH_2 [17].

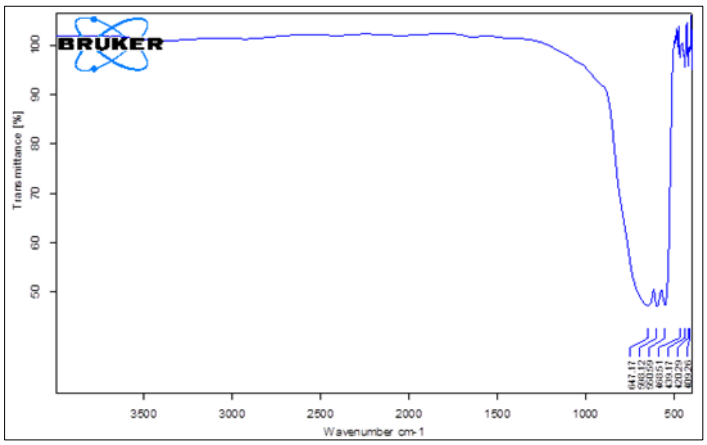

Fig 10: TiO2 (anatase) catalyst's ATR-FTIR spectrum

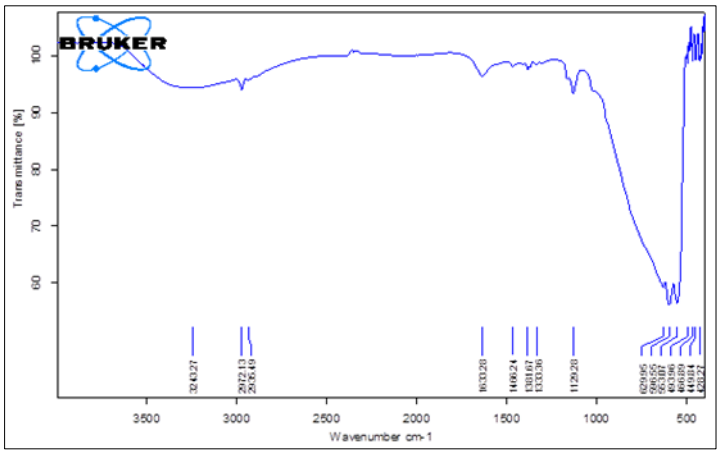

Fig 11: Catalyst N-doped TiO2's ATR-FTIR spectrum

3.2. UV-Vis Absorption Spectra

The ultraviolet and visible spectra revealed the absorption wavelength of the nitrogen-doped TiO2 catalyst, signifying the spectrum's straight line's end [18], as shown in Figure 12. The band gap was determined based on Planck's relation.

Table 1: energy band gap (Eg)

Type	λ	E_g	E_g
Titanium Dioxide	384 nm	5.2 x10^{-19} J	3.2 eV
Nitrogen-Doped Tio_2	482 nm	4.1 x10^{-19} J	2.5 eV

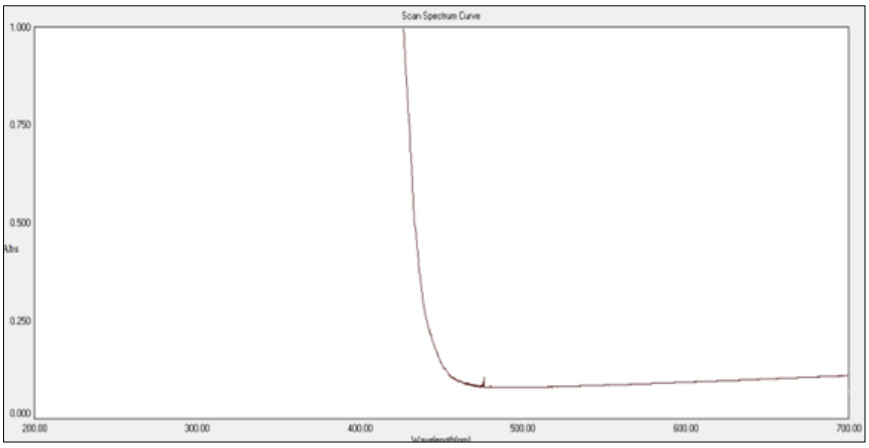

Fig 12: Catalyst nitrogen-doped TiO2's UV-visible spectrum

3.3. Catalyst Weight's Effect

The effect of TiO2 loading (mass) on the reaction's kinetics was also examined. The initial focus of 3-methyl phenol was fixed at 1x 10-4 mol. L-1, and TiO2 loading was used to track the initial rate of photodegradation (at constant initial concentration). Table (2) displays the results. Fig. 8 also displays the data. As anticipated, the initial rate of photocatalytic degradation of 3-methyl phenol increases with

increasing TiO2 load. The initial rate of deterioration (0.1 g.L-1) is predicted to decrease at greater TiO2 loading before becoming constant at higher TiO2 loading (0.43 g.L-1). The rate of photodegradation gradually slows down above this loading, which may be explained by the TiO2 suspension becoming more opaque to incident light. As a result, light absorption is restricted to the first layers of the photocatalytic mixture, with light photons not reaching the other layers of the solution. Additionally, light scattering becomes more efficient with high anatase loading, which lowers the photon intensity that TiO2 typically absorbs.

Table 2: The initial rate of 3- methyl phenol phtodegradation at various TiO2 loading.

Amount ($g.L^{-1}$)	0.10	0.25	0.35	0.43	0.51	0.59	0.67	0.75	0.83
P.D.E%	76	82	87	96	93	92	94	93	91

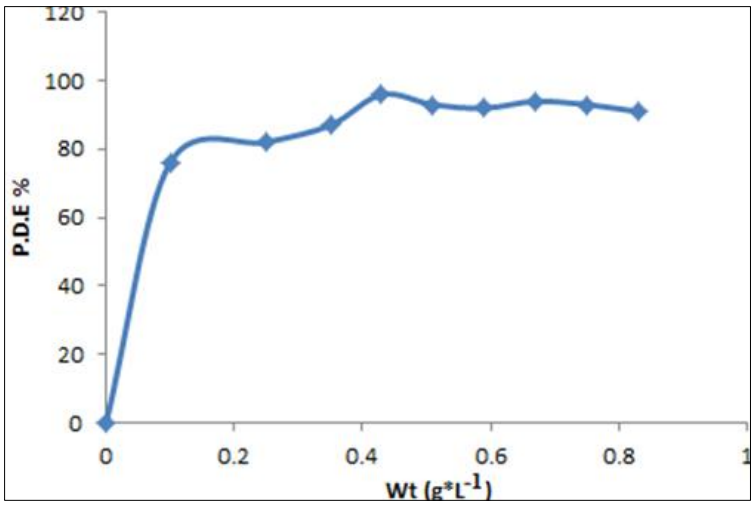

Fig 13: show optimized Weight of catalyst

3.4. Application TiO2 (anatase) and nitrogen-doped TiO2 on photodegradation of 3- methyl phenol compound under (UV) source and direct solar radiation.

3.4.1. UV source Irradiation

Following the photocatalytic breakdown of 3-methyl phenol under UV light and TiO2 (anatase), the compound's absorption spectra was monitored in an aqueous solution with an initial concentration of 1x10-4 moL.L-1, which had a λmax of 272 nm prior to irradiation. Using the catalyst's optimum weight (0.43 g.L-1), a drop in absorbance was seen after five minutes, as shown in Fig. 14.

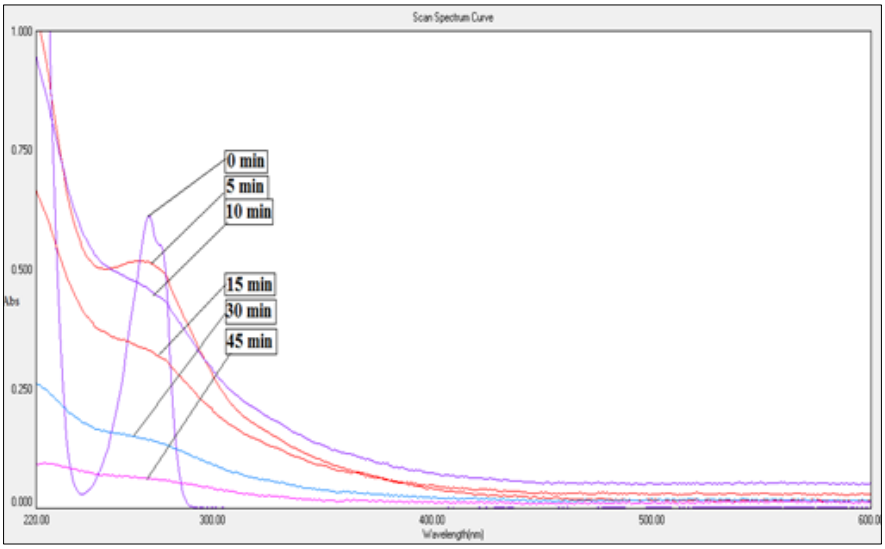

Fig 14: UV-visible spectra of 3-methyl phenol under a UV source using the catalyst TiO2 (anatase).

However, as shown in Fig. 10, substituting adopped TiO2 with nitrogen for the TiO2 (anatase) results in a noticeable decrease in absorbance in just two minutes as opposed to five minutes for undoped TiO2.

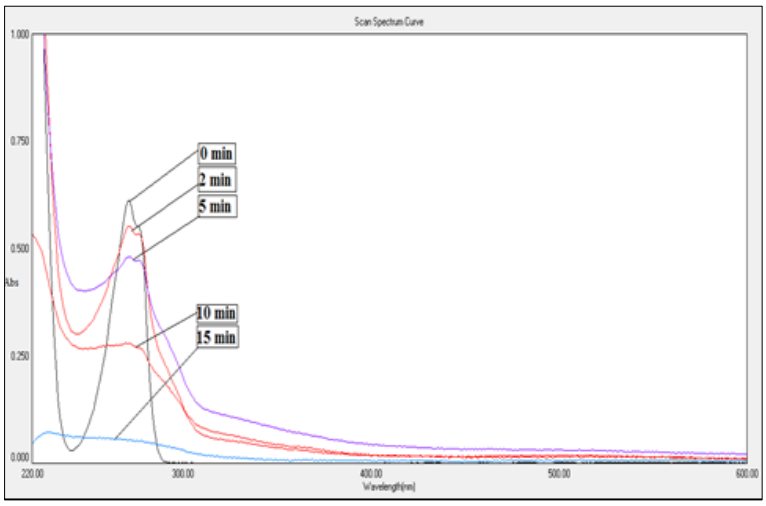

Fig 15: UV-visible spectra of 3-methyl phenol using N-doped TiO2 as a catalyst under a UV source.

3.4.2. Direct Solar Radiation

3-methyl phenol's photocatalytic breakdown in the presence of direct sunlight and TiO2 (anatase). Using the catalyst's optimum weight of 0.43 g.L-1, a drop in absorbance was observed after 200 minutes, as shown in Fig. 16.

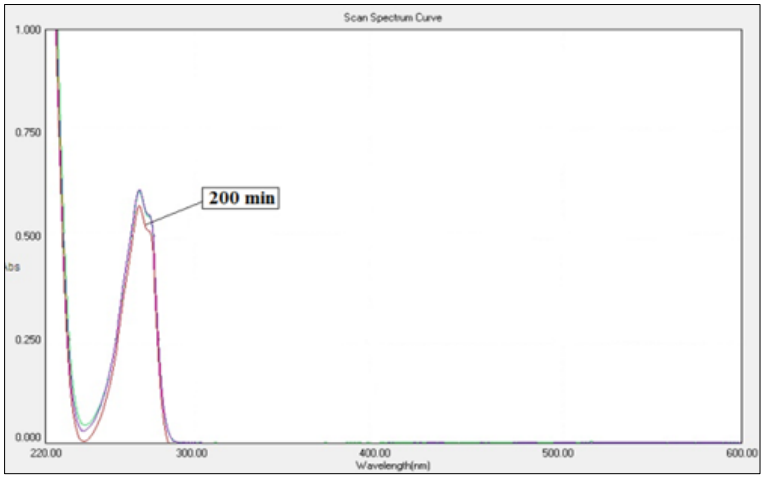

Fig 16: UV-visible spectra of 3-methyl phenol under direct sun light using the catalyst TiO2 (anatase)

Using the optimal weight of the catalyst N-doped TiO2, a decrease in absorbance was observed after 30 minutes, as shown in Fig. 17.

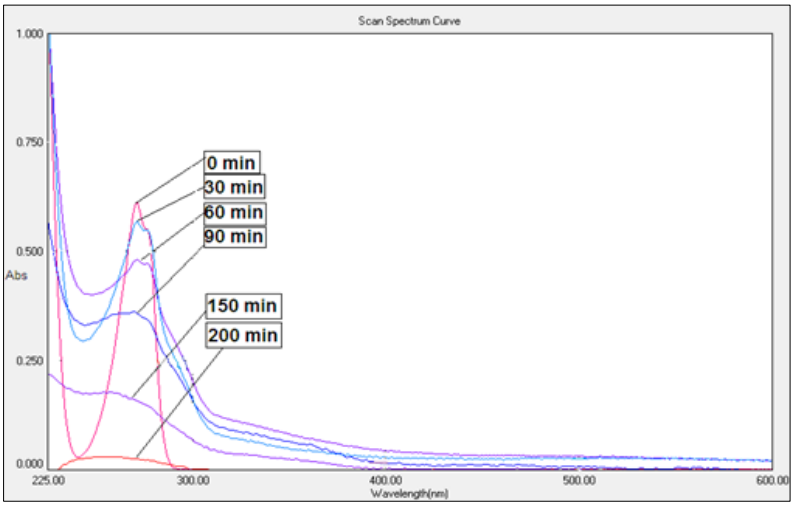

Fig 17: UV-visible spectra of 3-methyl phenol using nitrogen-doped TiO2 as a catalyst in direct sunlight.

4. Conclusions

1. The procedure that used and its modification lead to abtain of titanium dioxid with dimensionat nanometer.
2. Adoping by nitrogen atom led to decrease the band gap between valance band and
3. Conduction band for optical catalyst doped-TiO2.
4. We can be used sun light in order to reaction of photo degradation will be organic pollutauts.
5. The constant rate was high with catalyst N-doped TiO2.

References

1. Gaya UI, Abdullah AH. J Photochem Photobiol C Photochem. 2008;9.
2. Chen X, Mao SS. Chem Rev. 2007;107:2891.
3. Chatterjee D, Dasgupta S. J Photochem Photobiol C Photochem. 2005;6:186.
4. Klosek S, Raftery D. J Phys Chem B. 2001;105:2815.
5. Asahi R, Morikawa T, Ohwaki T, Aoki K, Taga Y. Visible-light photocatalysis in nitrogen-doped titanium oxides. Science. 2001;293(5528):269-271.
6. Gole JL, Stout JD, Burda C, Lou Y, Chen X. J Phys Chem B. 2004;108:1230.
7. Umebayashi T, Yamaki T, Tanaka S, Asai K. Chem Lett. 2003;32:330.
8. Khan S, Al-Shahry M, Ingler WB. Science. 2002;297:5590.
9. Li Q, Xue J, Liang W, Huang JH, Shang JK. Philos Mag Lett. 2008;88(3):231-238.
10. Sakai YW, Obata K, Hashimoto K, Irie H. Vacuum. 2008;83(3):683-687.
11. Irie H, Watanabe Y, Hashimoto K. J Phys Chem B. 2003:5483-5486.
12. Hashimoto K, Irie H, Fujishima A. Jpn J Appl Phys. 2005;44(12):8269-8285.
13. Almeida RM, Marques AC. Crystallization of sol-gel materials. In: SGT Annual Meeting Workshop on Crystallization; 2007 Sep 6-7; Derby.
14. Lam SM, Sin JC, Mohamed AR. Recent Pat Chem Eng. 2008;1:209-219.
15. Malato S, Blanco J, Vidal A, Richter C. Appl Catal B Environ. 2002;37:1-15.
16. Li X, Liu Q, Jiang XY, Huang J. Int J Electrochem Sci. 2012;7:11519-11527.
17. Chainarong S, Sikong L, Niyomwas S, Pavasupree S. In: Proceedings of the 9th Eco-Energy and Materials Science and Engineering Symposium; 2011; Chiang Rai, Thailand.
18. Joanna R, Anna I, Gerard S, Adriana Z. Physicochem Probl Miner Process. 2012;48:201-208.

How to Cite This Article

Mezaal FW. Modification the band gap of nano titanium dioxide and application its effectiveness on photodegradation of 3-methyl phenol. Int J Biol Biotechnol Res. 2026;2(4):34-42. doi:10.54660/IJBBR.2026.2.4.34-42.

Creative Commons (CC) License